Journal of Materials Chemistry C

First principles based screen for identification of transparent conductors

Journal:	*Journal of Materials Chemistry C*
Manuscript ID	TC-ART-11-2018-005917.R2
Article Type:	Paper
Date Submitted by the Author:	28-Jan-2019
Complete List of Authors:	Li, Yuwei; North China Institute of Aerospace Engineering; University of Missouri, Department of Physics and Astronomy Singh, David; University of Missouri, Department of Physics and Astronomy

Journal Name

ARTICLE TYPE

Cite this: DOI: 10.1039/xxxxxxxxxx

First principles based screen for identification of transparent conductors

Yuwei Li,[ab] David J. Singh*[b]

Received Date
Accepted Date

DOI: 10.1039/xxxxxxxxxx

www.rsc.org/journalname

We report a simple first principles based screen amenable to high throughput calculations for transparent conductors. These include the effects of doping on transparency, which can be important. In particular, doping leads to conduction accompanied by losses in transparency, both of which are materials dependent, but rarely considered in computational materials selection. We consider both the Drude contribution to optical conductivity, as well as new interband transitions that arise as a material is doped. This leads to a simple application dependent optical and electrical fitness function (OEF) that can be applied to semiconductors to identify materials that may be useful transparent conductors. The OEF goes beyond the frequently discussed criteria of suitable band gap and low effective mass. We illustrate this by application to a number of proposed p-type transparent conducting materials.

1 INTRODUCTION

Transparent conductors (TCs)[1], including transparent conducting oxides (TCOs)[2], combine optical transparency with electrical conductivity. They are widely used as electrodes in solar cell and display technologies.[3–8] The most commonly used material is Sn doped In_2O_3, known as ITO.[9–11] This is a stable n-type material that can be readily deposited in thin films. p-type TCs generally have lower performance in terms of the balance between conductivity and transparency.[12–15] Nonetheless, p-type TCs are highly desired for applications, e.g. for transparent electronics.[16] This has led to considerable effort in finding p-type TC materials, both experimentally and theoretically.[17–22]

Two requirements for a TC are a suitable optical band gap and sufficient mobility to be a conductor when doped. In general, materials with low hole effective mass, m_h^*, are most likely to have high mobility and conductivity when doped. Therefore several previous theoretical studies have focused on identification of materials with suitably wide band gaps and relatively low m_h^* as potential TCs.[19–29] However, doping, especially heavy doping, as is needed to obtain sufficient conductivity in TC materials, may lead to changes in the optical properties. This may be a Drude contribution from the carriers, which will lead to reflectivity and absorption,[30] especially in the infrared, but also in the red. There are proposals for reducing the Drude contribution, for example, using polaronic materials.[31] Additionally, electron correlations can affect the Drude weight by modifying the plasma frequency.[32] These effects are generally detrimental to the DC conductivity, and so it remains to be established whether they can be useful for TC performance.

There may also be interband transitions from occupied bands to the empty states at the top of the valence band in p-type doped material.[33,34] This phenomena, i.e. absorption due to interband transitions upon doping, has been termed a second gap. The effect of second gaps is strongly materials and doping level dependent. In particular, absorption due to a second gap depends in detail on the band structure through the joint density of states, and also on matrix elements. The light s-like conduction bands of many n-type TC materials can reduce the joint density of states, which works against strong absorption from interband transitions. In addition, there can be a change in the apparent optical gap, often to higher values, due to the Burstein-Moss effect, but sometimes to lower values due to doping induced changes in band structure or disorder induced tails in spectra.

Finally, it should be noted that for each application there is a desired spectral range for transparency. For example, the band gaps of Si and CdTe are 1.1 eV and 1.5 eV, which are in the infrared, meaning that efficiency of solar cells will benefit from transmission of this near IR light. Displays, on the other hand, typically do not have red emission below 1.9 eV, and therefore transparency below 1.8 eV or 1.9 eV, is not needed, and may even be undesirable. As discussed in more detail below, we find that the ordering of materials in terms of anticipated performance is significantly different for different applications.

[a] North China Institute of Aerospace Engineering, No. 133 Aimin East Road , Langfang, Hebei 065000, China
[b] Department of Physics and Astronomy, University of Missouri, Columbia, MO 65211-7010 USA
*E-mail: singhdj@missouri.edu

† Electronic Supplementary Information (ESI) available: See DOI: 10.1039/b000000x/

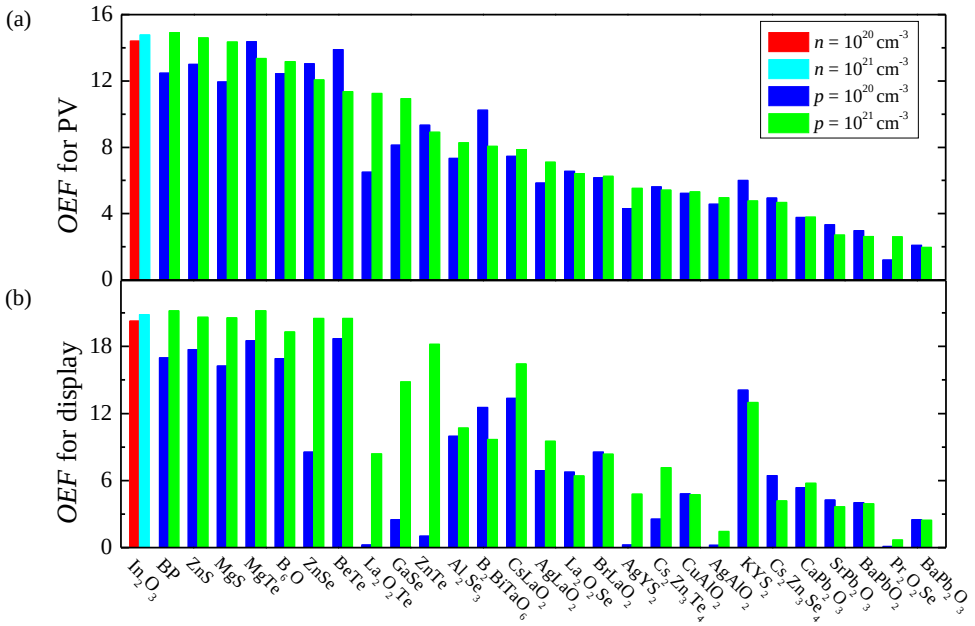

Fig. 1 Optical and electrical fitness function (OEF) of the wide bandgap semiconductors considered. Note that some high performance PV materials, have low fitness for the display scenario. n-type In_2O_3 is also shown.

Here, we present simple application dependent screens, or optical and electrical fitness functions, that can be used to assess potential TC performance in a given application context, based on results from first principles calculations. To illustrate these, we consider two notional applications. These are a Si solar cell for which high transparency is needed from 1.2 eV to 2.5 eV and a display for which transparency is important from 1.8 to 3.0 eV, and investigate several previously proposed p-type TC materials in this context. We note that experimental testing of compounds as TCs is challenging, for example, due to the need for suitable doping. As a result, a number of the materials investigated here have not yet been experimentally tested.

We find that there are differences in the materials that are most promising for these two application scenarios, even among high gap materials that without doping would be fully transparent over the entire range for both applications. The materials limitations embodied in our screens come from the balance between reduced transparency as the materials are doped and the conductivity that arises from the doping. Both of these are strongly material dependent. The analysis also provides an explanation for why there are relatively few known p-type TC materials with good performance, even though there are many compounds with suitable band gaps and reasonable effective masses.

2 COMPUTATIONAL METHODS

Our first principles calculations were performed within density functional theory. We used methods that yield band gaps close to experimental values for the calculation of optical properties, as discussed below. p-type doping was treated using the virtual crystal approximation. The virtual crystal approximation is an average potential approximation that goes beyond the rigid band approximation in that it includes doping dependent changes in band structure. The electronic structures were obtained with the general potential linearized augmented plane wave (LAPW) method as implemented in the WIEN2k code.[35,36] The accurate electronic structures on dense grids in the Brillouin zone that are available from this approach facilitate the optical and electronic transport calculations. A basis set cutoff K_{max} determined by the criterion $R_{min}K_{max} \geq 7.0$ was used for oxides and $R_{min}K_{max} = 9.0$ was used for non-oxides. Here, R_{min} denotes the smallest LAPW sphere radius among the atoms in the unit cell. In the oxides we used oxygen sphere radii smaller than the metal radii. This leads to higher effective RK_{max} values for the metal atoms, similar to the values used in the non-oxides. We did optical calculations including a Drude contribution.

We used the GGA+U method[37,38] for phases with d or f orbitals, such as those containing Cu^+, Ag^+ and Pr^{3+} ions. The value of the parameter U was determined based on hybrid functional calculations with the HSE06 functional.[39,40] The modified Becke-Johnson (mBJ) potential of Tran and Blaha[41,42] was used for the other phases. The mBJ potential gives band gaps in generally good accord with experiment for a wide variety of simple semiconductors and insulators.[23,43,44] We fixed the lattice parameters to the experimental values and relaxed internal atomic coordinates. Spin-orbit coupling (SOC) was included in the electronic structure calculations.

The Drude contribution to the real part of the optical conductivity was obtained using the calculated plasma frequencies, Ω_p. These were calculated using the virtual crystal approximation electronic structures of the doped materials. The Drude calculation also requires a broadening, which is related to the scattering time. We used the same broadening for all materials, $\gamma \approx 1.52$ eV. This is the value from experiments on ITO with carrier concentration, n=1.4×10^{21} cm^{-3}.[45] This amounts to setting the scattering time the same for all compounds. This is clearly a rough estimate, but has the advantage of allowing comparison of different materi-

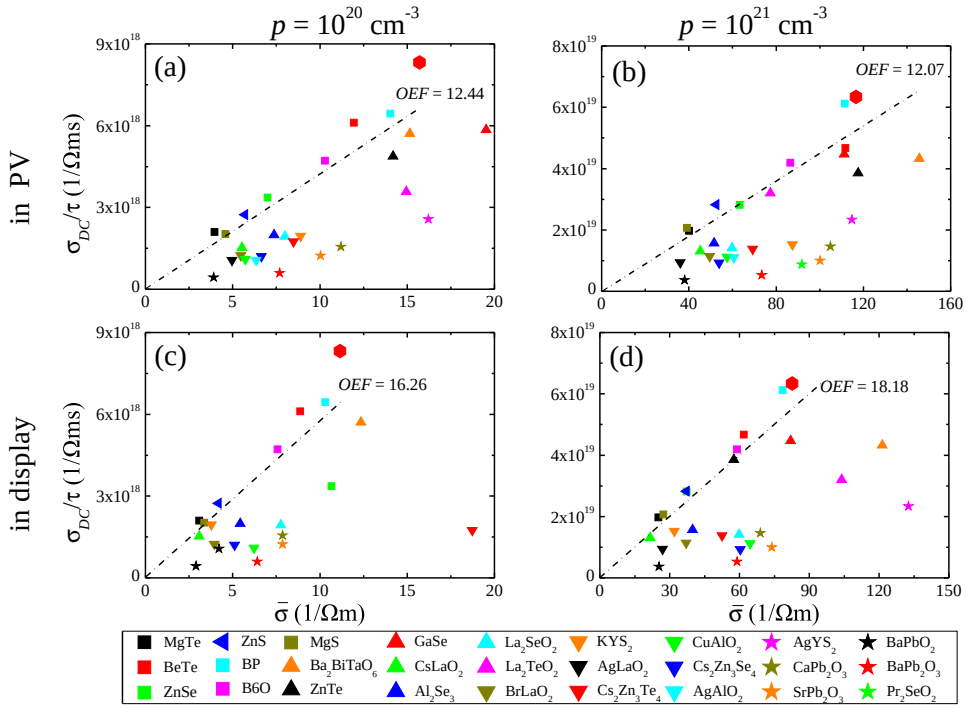

Fig. 2 Calculated σ_{DC}/τ vs. $\overline{\sigma_{opt}}$ at p=10^{20} and p=10^{21} cm^{-3} for applications in PV and display respectively. Note that the points for ZnS and ZnSe in panel (d) are practically coincident. n-type In_2O_3 is also shown (filled red hexagon). Reference lines are given as a guide to the eye (see text).

als from an electronic structure point of view. It also captures the expectation that high carrier mass will harm the conductivity of a material, while also reducing the Drude absorption, which may partially compensate this degradation.

We used the transport effective mass to characterize the values of m_h^* for these heavily doped materials. The reason is that several of these materials have complex band structures, with multiple bands at or close to the valence band extrema. There are also anisotropic non-parabolic band dispersions among the materials. Use of the transport effective mass amounts to calculating the value of m_h^* that in a parabolic band model would yield that same value of the transport coefficient σ_{DC}/τ as the value obtained the actual detailed band structure of the material. This yields values of m_h^* that can depend on doping. This has been discussed in the context of thermoelectrics where complex non-parabolic band structures can be favorable for high thermoelectric performance.[46] We find that this variation with doping is quite significant in some materials, e.g. Pr_2SeO_2, reflecting the complex non-parabolic band structure (see supplementary information).

We used the BoltzTraP code[47] with the procedure of transM[23,48] for this purpose. This takes into account effects of non-parabolicity and anisotropy of bands, multiple minima and multiple bands, etc. on carrier transport, and yields values appropriate for characterizing conductivity.

3 RESULTS and DISCUSSION

It is highly desirable to use a material dependent figure of merit that does not make assumptions about engineering choices. This is in order to rank different potential p-type TC materials in terms of performance. The present work is based on the ratio of the DC to the real part of the optical conductivity, σ_{DC}/σ_{opt}. This does not require assumptions about the film thickness and other engineering parameters. For example, some applications may require greater transparency, and others greater conductivity or mobility. These can be tuned by film thickness, doping level and materials selection. Our work focuses on materials selection. We then construct an optical and electrical fitness function, $OEF = \sigma_{DC}/\overline{\sigma_{opt}}$, where $\overline{\sigma_{opt}}$ is the average real part of the optical conductivity over an energy range, E_1 – E_2, of interest. It should be noted that optical conductivity and absorption coefficient are closely related. In terms of the complex frequency dependent dielectric function, $4\pi \mathrm{Re}(\sigma(\omega)) = \omega\, \mathrm{Im}(\varepsilon(\omega))$. The absorption coefficient is $\alpha = 2\omega k/c$, where k is the extinction, $k = \mathrm{Im}(\varepsilon^{1/2}(\omega))$.

To proceed, we approximate the σ_{opt} by the calculated interband contributions for the doped material plus a Drude form based on the calculated plasma frequency and an assumed width. For σ_{DC} we use a calculated σ_{DC}/τ based on the band structure with a constant assumed scattering time consistent with the assumed width in the Drude formula. σ_{DC}/τ can be obtained directly from band structure.[47] The use of the same scattering for the DC conductivity and the Drude part of the optical conductivity leads to a partial cancellation that weakens the dependence of the OEF on τ. The OEF captures the band structure dependent part of the figure of merit. We illustrate this doping level dependent function by calculations for doping levels of p=10^{20} cm^{-3} and p=10^{21} cm^{-3}. We take the energy ranges (E_1 – E_2) as 1.2 – 2.5 eV and 1.8 – 3.0 eV for the photovoltaic (PV) and display application scenarios, respectively. In practice, one might decide on the spectral range of importance for the specific application,

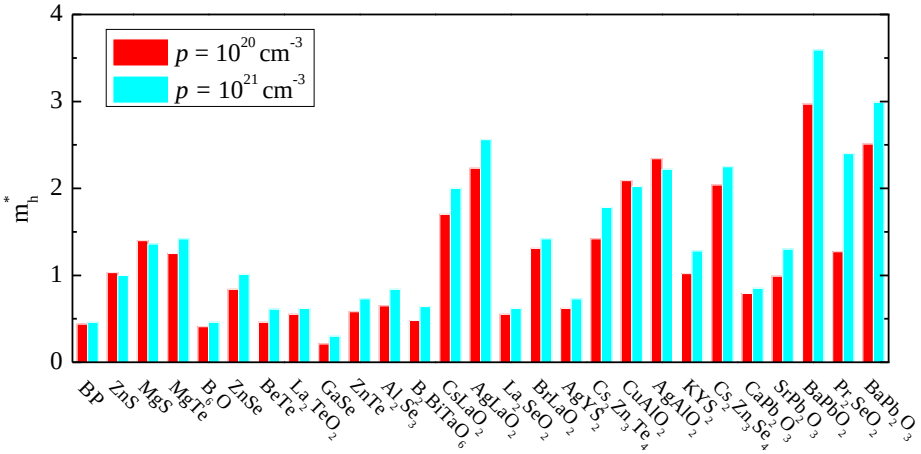

Fig. 3 Transport effective mass, m_h^* in the lowest mass direction at p=10^{20} and p=10^{21} cm^{-3}. This is motivated by the fact that some the known high performance p-type TCO materials, especially delafossites are highly anisotropic.

and then calculate the OEF, to identify materials for that application. One could also in principle generalize this by introducing a weight function into the spectral average, for example based on the solar spectrum and the characteristics of the absorber material in a PV application. In any case, the larger the OEF, the better the likely performance.

The main approximations made are in the very simple choice of τ, which controls the Drude width, in the simple Drude form used, and in the calculation of interband transitions with the independent particle dipole approximation. It also depends on the accuracy of the band structure upon which it is based.

We note that the optical and transport properties entering the OEF are obtainable at reasonable computational cost. The main requirement is a virtual crystal self-consistent calculation at each doping level, followed by an optical calculation. Generally, the computational load for an optical calculation is a small fraction of that in the self-consistent calculation.

The advantages are that the OEF is sufficiently simple to be implemented in high throughput fashion, it incorporates key physics, and it does not rely on experimental information. Finally, we note that it is important to fully characterize materials using experimental synthesis, chemical doping, and optimization of growth conditions in order to develop new TCs. For example, it is important to determine what doping levels can be obtained in a given material under feasible growth conditions. The purpose of the OEF is to provide an indication of which materials are most promising. It is hoped that this can be useful for focusing experimental work on more favorable compounds, and for finding new potential TC materials among compounds that have not been previously studied in this context.

We begin with discussion of the main results, i.e. the OEF of different materials, and then discuss the properties of individual materials. The OEF are shown in Fig. 1, and are listed in Table S1. We note first of all that the OEF values do distinguish between different materials. Secondly, it is important to note that the calculated OEF depends significantly on the spectral range, and that that rankings of the materials are different for the two application scenarios. Finally, the OEF depends strongly on the doping level. This emphasizes the importance in practice of optimizing the doping level to obtain the highest TC performance in a given material. It also underscores the limitations of screens based only on properties of the undoped material, as these do not include the effects of different doping levels. Widely used, n-type In_2O_3 is also shown for comparison. As seen, it is the best material in the doping range where it is used. In_2O_3 combines high OEF with ready doping via Sn substitution, reasonably high static dielectric constant (favorable for conductivity with heavy doping),[49] stability and facile growth of high quality films.

Fig. 2 shows the components of the OEF, σ_{DC}/τ vs. $\overline{\sigma_{opt}}$ at p=10^{20} and p=10^{21} cm^{-3}. As seen, these are correlated. This is as may be expected since both contain the plasma frequency, In addition, a number of materials show lower performance relative to that expected from this correlation. This is due mainly to interband transitions, as discussed below. The existence of these compounds with lower OEF shows the value of the OEF in addition to the effective mass and band gap. In particular, it shows that some materials with suitable band gap and effective mass show distinctly lower performance, and therefore would be removed in a down-selection based on OEF. We note that experimental development of a new TC is very challenging, and in particular faces challenges such as finding ways of doping materials and producing high quality doped films. Therefore theory based down-selections can be valuable.

Since the OEF is the ratio of the two quantities, we plot also reference lines indicating values for compounds that are considered high performance p-type TCs. This line is a guide to the eye that separates low OEF materials from higher OEF materials that may have superior performance. Hole effective masses in the lowest effective mass direction are given in Fig. 3.

Importantly, there are quite a number of materials that would seemingly have properties that would make them good TCs based on the characteristics of the undoped phase, but in fact have low OEF, as seen by their position well below the reference lines. This supports the usefulness of the OEF as a screen, and also provides

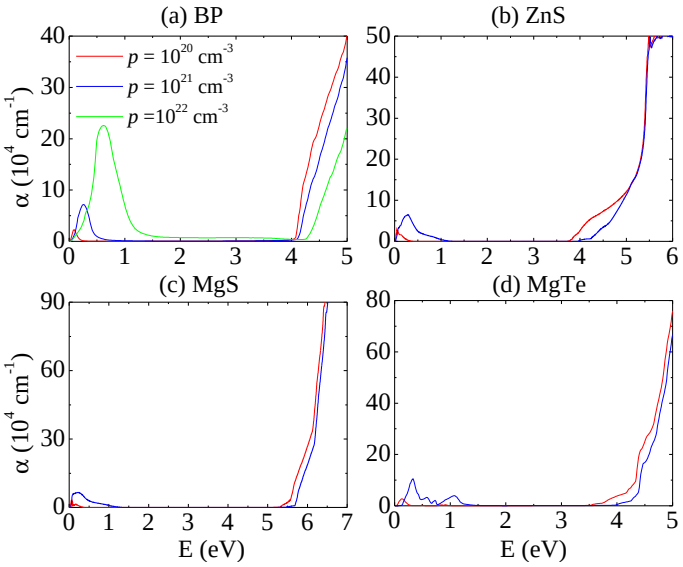

Fig. 4 The absorption spectra of (a) BP, (b) ZnS, (c) MgS and (d) MgTe at p=10^{20} and p=10^{21} cm^{-3} respectively. The absorption spectrum of BP at p=10^{22} cm^{-3} is also shown.

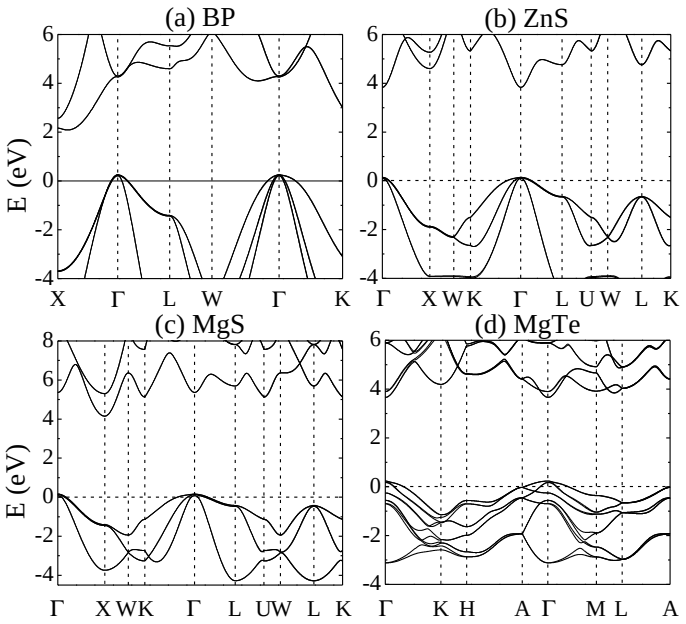

Fig. 5 The band structures of (a) BP, (b) ZnS, (c) MgS and (d) MgTe at p=10^{21} cm^{-3}. The Fermi levels are at 0 eV.

an explanation for why there are relatively few TC materials, even though many materials have suitable band gaps. Such screens (or filters) are important because experimental development of TC materials is very challenging due to the frequent difficulties in obtaining heavy doping in wide gap materials, as well as in growing high quality films of these doped materials.

We find that BP, ZnS, MgS and MgTe are favorable potential p-type TCs based on the calculated OEF. They have low m_h^* ($<$ 1.5 m$_0$) and low absorption in the visible, as seen in Fig. 3 and Fig. 4. Their band structures at p=10^{21} cm^{-3} are given in Fig. 5. MgTe does have a second gap that can lead to absorption, but its energy is in the infrared, and therefore it does not contribute to visible absorption. This second gap is associated with interband transitions near the zone center, Γ. Additionally at sufficiently high doping transitions can open in other parts of the zone, particularly A. This is the key to their high visible transparency under doping. For comparison, the band structures of Ca/Sr/BaPb$_2$O$_3$ and BaPbO$_2$ are given in Fig. S1. These do have second gaps with visible absorption and this leads to lower OEF. These second gaps are a consequence of the many bands that are close to the valence band maximum. It is worth noting that some materials, such as BP, still maintain high performance under high doping conditions, as seen the green lines in the Fig. 4 (a). BP still maintains visible transparency at p=10^{22} cm^{-3}. Turning to differences between applications, it is seen that performance as measured by the OEF in a given material can be significantly different in PV and display applications. Examples are ZnSe, La$_2$TeO$_2$, GaSe and ZnTe. Also they can be quite different at different doping levels, for example, ZnSe, GaSe, ZnTe and AgYS$_2$. To explain this we show the band structures of La$_2$TeO$_2$ and ZnTe at p=10^{20} and p=10^{21} cm^{-3}, in Fig. 6.

La$_2$TeO$_2$ is an instructive case. The direct band gap of La$_2$TeO$_2$ is ∼2.5 eV. This would seem sufficient for our PV scenario, but not for the display scenario. p-type doping increases the effective optical gap via the Burstein-Moss effect (red arrows in Fig. 6(a)). This then improves the optical performance, even in the display scenario. Thus the OEF at p=10^{21} cm^{-3} is better than at p=10^{20} cm^{-3}. However, the Burstein-Moss effect is relatively small for materials with high effective mass, i.e. high density of states near the band edge, which is the case for La$_2$TeO$_2$.

In addition, there is interband absorption in the visible due to transitions, as indicated by the blue arrow in Fig. 6 (b). This affects the transparency, especially with heavy doping. p-type ZnTe has a stronger Burstein-Moss shift than La$_2$TeO$_2$, as shown by the blue arrow in the Fig. 6 (c) and (d). Also, distinct from La$_2$TeO$_2$, ZnTe does not have any second gap in the visible, even with heavy doping, as indicated by the red arrow in Fig. 6 (c). Thus ZnTe maintains favorable properties with heavy doping. The band structures and absorption spectra of other phases are given in the supplementary information.

4 SUMMARY and CONCLUSIONS

We used first-principles calculations to study the optical and electronic properties of doped p-type materials that have been proposed as TCs in prior work. We propose a simple fitness function, the OEF, that couples the electrical conductivity and optical properties as a simple band structure based screen.

The key ingredient in the OEF beyond the screening based on undoped materials has to do with the fact that in some materials, but not others, the transparency is strongly reduced by doping. However, doping is essential for conductivity, and again the relationship between carrier concentration produced by doping and conductivity is material dependent. The OEF is a screen that can be readily calculated from standard first principles calculations and incorporates these effects in addition to requirements, such as band gap, that can be obtained without consideration of doping. It would be of interest to further validate this approach by

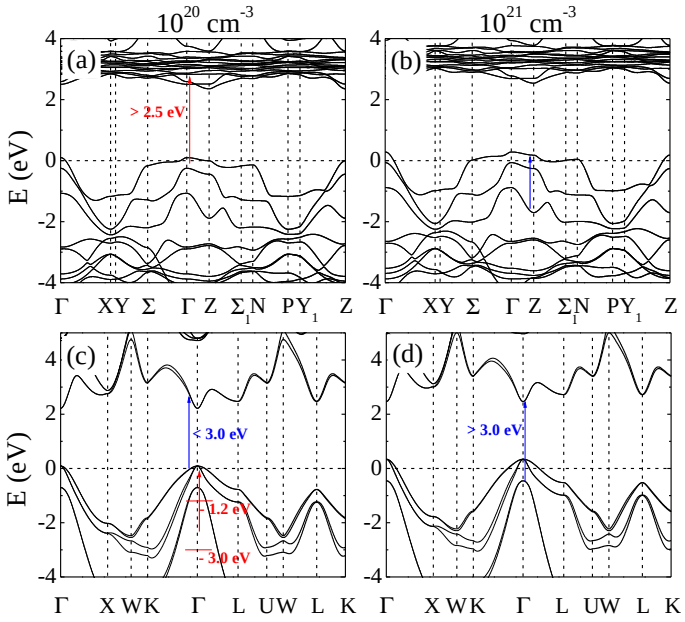

Fig. 6 Band structures of La_2TeO_2 (top, (a) and (b)) and ZnTe (bottom, (c) and (d)) at p=10^{20} (left, (a) and (c)) and p=10^{21} cm^{-3} (right, (b) and (d)). In each case the Fermi energy is at 0 eV.

parametric experimental studies of conductivity and absorption spectra in relation to calculated *OEF* values for different classes of proposed *p*-type TC materials.

We find that many of the proposed materials have high *OEF*, but that certain compounds, mostly those characterized by so-called second gaps, do not. We also note that the performance depends significantly on the spectral range needed for the application. This is a fact that should be kept in mind when seeking new TC materials.

Finally, it should be emphasized that it is important to fully characterize materials using experimental synthesis, chemical doping, and optimization of growth conditions in order to develop new TC. The purpose of the *OEF* is to provide an indication of which materials are promising. It is hoped that this can be used to focus expensive experimental work on more favorable compounds.

ACKNOWLEDGMENTS

This work was supported by the Department of Energy, Office of Science, Basic Energy Sciences, MAGICS Center, Award DE-SC0014607.

References

1 K. L. Chopra, S. Major and D. K. Pandya, *Thin Solid Films*, 1983, **102**, 1–46.
2 A. Stadler, *Mater.*, 2012, **5**, 661–683.
3 H. Kawazoe, H. Yanagi, K. Ueda and H. Hosono, *MRS Bull.*, 2000, **25**, 28–36.
4 F. N. Ishikawa, H.-K. Chang, K. Ryu, P.-C. Chen, A. Badmaev, L. Gomez De Arco, G. Shen and C. Zhou, *ACS Nano*, 2009, **3**, 73–79.
5 K. Nomura, H. Ohta, A. Takagi, T. Kamiya, M. Hirano and H. Hosono, *Nature*, 2004, **432**, 488–492.
6 H. Chiang, J. Wager, R. Hoffman, J. Jeong and D. A. Keszler, *Appl. Phys. Lett.*, 2005, **86**, 013503.
7 D. S. Ginley and C. Bright, *MRS Bull.*, 2000, **25**, 15–18.
8 M. Morales-Masis, S. De Wolf, R. Robinson-Woods, J. W. Ager and C. Ballif, *Adv. Electronic Mater.*, 2017, **3**, 1600529.
9 H. Hartnagel, A. Dawar, A. Jain and C. Jagadish, *Semiconducting transparent thin films*, Institute of Physics Bristol, 1995.
10 T. Minami, *Thin Solid Films*, 2008, **516**, 5822–5828.
11 M. Veith, B. Rabung, I. Grobelsek, M. Klook, F. E. Wagner and M. Quilitz, *J. Nanosci. Nanotechnol.*, 2009, **9**, 2616–2627.
12 T. Minami, *MRS Bull.*, 2000, **25**, 38–44.
13 S. Sheng, G. Fang, C. Li, S. Xu and X. Zhao, *Phys. Status Solidi A*, 2006, **203**, 1891–1900.
14 Z. Wang, P. K. Nayak, J. A. Caraveo-Frescas and H. N. Alshareef, *Adv. Mater.*, 2016, **28**, 3831–3892.
15 R. Nagarajan, A. D. Draeseke, A. W. Sleight and J. Tate, *J. Appl. Phys.*, 2001, **89**, 8022–8025.
16 A. Liu, H. Zhu, W. T. Park, S. J. Kang, Y. Xu, M. G. Kim and Y. Y. Noh, *Adv. Mater.*, 2018, **30**, 1802379.
17 K. H. L. Zhang, K. Xi, M. G. Blamire and R. G. Egdell, *J. Phys.: Condens. Matter*, 2016, **28**, 383002.
18 K. Fleischer, E. Norton, D. Mullarkey, D. Caffrey and I. V. Shvets, *Materials*, 2017, **10**, 1019.
19 J. Varley, V. Lordi, A. Miglio and G. Hautier, *Phys. Rev. B*, 2014, **90**, 045205.
20 N. Sarmadian, R. Saniz, B. Partoens and D. Lamoen, *Sci. Rep.*, 2016, **6**, 20446.
21 K. Bhamu and K. Priolkar, *Mater. Chem. Phys.*, 2017, **190**, 114–119.
22 J. Shi, T. F. Cerqueira, W. Cui, F. Nogueira, S. Botti and M. A. Marques, *Sci. Rep.*, 2017, **7**, 43179.
23 Y. Li, L. Zhang and D. J. Singh, *Phys. Rev. Mater.*, 2017, **1**, 055001.
24 T. F. Cerqueira, S. Lin, M. Amsler, S. Goedecker, S. Botti and M. A. Marques, *Chem. Mater.*, 2015, **27**, 4562–4573.
25 H. Shi, B. Saparov, D. J. Singh, A. S. Sefat and M.-H. Du, *Phys. Rev. B*, 2014, **90**, 184104.
26 K. Yim, Y. Youn, M. Lee, D. Yoo, J. Lee, S. H. Cho and S. Han, *npj Comput. Mater.*, 2018, **4**, 17.
27 A. Bhatia, G. Hautier, T. Nilgianskul, A. Miglio, J. Sun, H. J. Kim, K. H. Kim, S. Chen, G.-M. Rignanese, X. Gonze *et al.*, *Chem. Mater.*, 2015, **28**, 30–34.
28 J. B. Varley, A. Miglio, V.-A. Ha, M. J. van Setten, G.-M. Rignanese and G. Hautier, *Chem. Mater.*, 2017, **29**, 2568–2573.
29 R. K. M. Raghupathy, T. D. Kühne, C. Felser and H. Mirhosseini, *J. Mater. Chem. C*, 2018, **6**, 541–549.
30 I. Hamberg and C. G. Granqvist, *J. Appl. Phys.*, 1998, **60**, R123.
31 G. Brunin, G. M. Rignanese and G. Hautier, *cond-mat*, unpublished, arXiv:1810.04919.
32 M. M. Qazilbash, J. J. Hamlin, R. E. Baumbach, L. Zhang, D. J.

Singh, M. B. Maple and D. N. Basov, *Nature Physics*, 2009, **5**, 647.
33 Y. Li, L. Zhang, Y. Ma and D. J. Singh, *APL Mater.*, 2015, **3**, 011102.
34 V.-A. Ha, D. Waroquiers, G.-M. Rignanese and G. Hautier, *Appl. Phys. Lett.*, 2016, **108**, 201902.
35 D. J. Singh and L. Nordstrom, *Planewaves, Pseudopotentials, and the LAPW method*, Springer Science & Business Media, 2006.
36 P. Blaha, K. Schwarz, G. K. H. Madsen, D. Kvasnicka and J. Luitz, *WIEN2k, An augmented plane wave+ local orbitals program for calculating crystal properties*, 2001.
37 J. P. Perdew, K. Burke and M. Ernzerhof, *Phys. Rev. Lett.*, 1996, **77**, 3865.
38 A. I. Liechtenstein, V. I. Anisimov and J. Zaanen, *Phys. Rev. B*, 1995, **52**, R5467.
39 J. Heyd, G. E. Scuseria and M. Ernzerhof, *J. Chem. Phys.*, 2003, **118**, 8207–8215.
40 J. Heyd, G. E. Scuseria and M. Ernzerhof, *J. Chem. Phys.*, 2006, **124**, 219906.
41 F. Tran and P. Blaha, *Phys. Rev. Lett.*, 2009, **102**, 226401.
42 D. Koller, F. Tran and P. Blaha, *Phys. Rev. B*, 2011, **83**, 195134.
43 Y. Li, J. Sun and D. J. Singh, *Appl. Phys. Lett.*, 2017, **110**, 051904.
44 Y. Li and D. J. Singh, *Phys. Rev. Mater.*, 2017, **1**, 075402.
45 X. Liu, J. Park, J.-H. Kang, H. Yuan, Y. Cui, H. Y. Hwang and M. L. Brongersma, *Appl. Phys. Lett.*, 2014, **105**, 181117.
46 G. Xing, J. Sun, Y. Li, X. Fan, W. Zheng and D. J. Singh, *Phys. Rev. Materials*, 2017, **1**, 065405.
47 G. K. H. Madsen and D. J. Singh, *Comput. Phys. Commun.*, 2006, **175**, 67–71.
48 transM code, faculty.missouri.edu/singhdj/transm.shtml.
49 X. He, D. J. Singh, P. Boon-on, M. W. Lee and L. Zhang, *J. Am. Chem. Soc.*, 2018, **140**, 18065.

TOC Graphic and Sentence of Text:

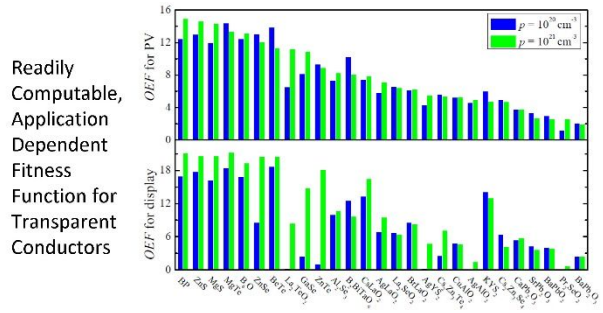

We present methods for screening semiconductors as transparent conductors leading to a simple application dependent fitness function.